Oncogene (2018) 37:3998–4012
https://doi.org/10.1038/s41388-018-0147-x

ARTICLE

Lymphomas driven by Epstein–Barr virus nuclear antigen-1 (EBNA1) are dependant upon Mdm2

Sana AlQarni[1] · Yazeed Al-Sheikh[1,2] · Donald Campbell[1] · Mark Drotar[1] · Adele Hannigan[1,3] · Shelagh Boyle[4] · Pawel Herzyk[1] · Andrew Kossenkov[5] · Kate Armfield[1] · Lauren Jamieson[1] · Mariarca Bailo[1] · Paul M. Lieberman[5] · Penelope Tsimbouri[1] · Joanna B. Wilson[1]

Received: 20 September 2017 / Revised: 7 December 2017 / Accepted: 19 December 2017 / Published online: 25 April 2018

Abstract

Epstein–Barr virus (EBV)-associated Burkitt's lymphoma is characterised by the deregulation of c-Myc expression and a restricted viral gene expression pattern in which the EBV nuclear antigen-1 (EBNA1) is the only viral protein to be consistently expressed. EBNA1 is required for viral genome propagation and segregation during latency. However, it has been much debated whether the protein plays a role in viral-associated tumourigenesis. We show that the lymphomas which arise in EμEBNA1 transgenic mice are unequivocally linked to EBNA1 expression and that both C-Myc and Mdm2 deregulation are central to this process. Tumour cell survival is supported by IL-2 and there is a skew towards CD8-positive T cells in the tumour environment, while the immune check-point protein PD-L1 is upregulated in the tumours. Additionally, several isoforms of Mdm2 are upregulated in the EμEBNA1 tumours, with increased phosphorylation at ser166, an expression pattern not seen in Eμc-Myc transgenic tumours. Concomitantly, E2F1, Xiap, Mta1, C-Fos and Stat1 are upregulated in the tumours. Using four independent inhibitors of Mdm2 we demonstrate that the EμEBNA1 tumour cells are dependant upon Mdm2 for survival (as they are upon c-Myc) and that Mdm2 inhibition is not accompanied by upregulation of p53, instead cell death is linked to loss of E2F1 expression, providing new insight into the underlying tumourigenic mechanism. This opens a new path to combat EBV-associated disease.

Introduction

The human gammaherpesvirus Epstein–Barr virus (EBV) is causally associated with several malignancies of epithelial and B-cell origin, including nasopharyngeal carcinoma and Burkitt's lymphoma (BL). The Epstein–Barr virus nuclear antigen 1 (EBNA1) is a multifunctional DNA binding protein which is essential for the lifelong persistence of the virus in the host. It plays a vital role in viral genome replication and is required for efficient mitotic segregation during latent infection [1]. The protein also acts as a transcriptional regulator of both viral and host promoters [2]. EBNA1 achieves its functions by binding to viral and host DNA, host proteins and RNA [3, 4]. In addition, it was recently discovered that the gly/ala repeat (GAr) region of EBNA1 that mediates translation suppression leads to a stress response which promotes E2F1 translation [5].

While clearly pleiotropic, the role of EBNA1 in EBV-associated malignancies has remained enigmatic. We previously reported that B-cell-directed expression of EBNA1 predisposed transgenic mice to B-cell lymphoma,

Electronic supplementary material The online version of this article (https://doi.org/10.1038/s41388-018-0147-x) contains supplementary material, which is available to authorized users.

✉ Joanna B. Wilson
Joanna.wilson@glasgow.ac.uk

1 College of Medical, Veterinary and Life Sciences, University of Glasgow, Glasgow G12 8QQ, UK

2 Present address: College of Applied Medical Sciences, King Saud University, Riyadh, Saudi Arabia

3 Present address: TCBiopharm, Maxim1, 2 Parklands Way Holtown, Motherwell ML1 4WR UK

4 MRC Human Genetics Unit, Institute of Genetics and Molecular Medicine, University of Edinburgh, Edinburgh EH4 2XU, UK

5 Center for Chemical Biology and Translational Medicine, The Wistar Institute, 3601 Spruce Street, Philadelphia, PA 19104, USA

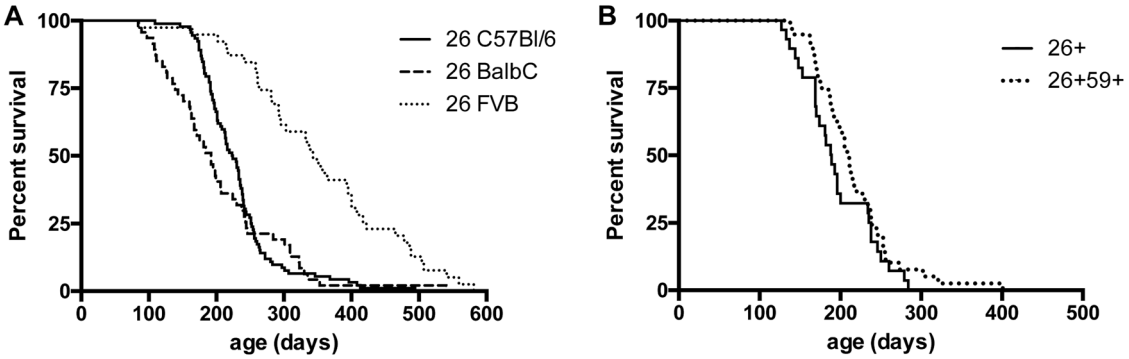

Fig. 1 The EμEBNA1.26 lymphoma phenotype persists in different strain backgrounds. **a** The lymphoma incidence in EμEBNA1.26 mice in the strain background of C57Bl/6 ($n = 75$) was compared after crossing the transgene for at least 5 generations (>96.875% backcross strain) to mouse strain BalbC ($n = 47$) and FVB ($n = 39$). EμEBNA1.26 mice of strain BalbC started to develop B-cell lymphoma at a slightly earlier age (median 192 days) compared to the C57Bl/6 strain (median 223 days) and displayed greater lymph node involvement, while mice of strain FVB showed a longer latency to B-cell lymphoma development (median 339 days). **b** Mice of lines EμEBNA1.26 and EμEBNA1.59 (both in C57Bl/6 strain) were crossbred and the lymphoma incidence compared between bi-transgenic ($26 + 59 +$, $n = 39$) and single EμEBNA1.26 positives ($26+$, $n = 29$) revealing no difference

suggesting a direct role for the protein in lymphoid malignancies, particularly BL [6]. In two transgenic lines expressing the transgene, we showed a curious inverse relationship between the level of EBNA1 protein and the incidence of lymphoma.

There is now considerable evidence to support the hypothesis that EBNA1 has oncogenic activity. Inhibition of EBNA1 decreases the survival of EBV-positive BL cells and it was shown that EBNA1 could inhibit p53-mediated apoptosis [7]. Further, EBNA1 interacts with the ubiquitin-specific protease USP7, an enzyme which removes ubiquitin groups from its target proteins, which include both p53 and Mdm2 [8]. EBNA1 has been shown to induce several transcription factors that regulate pathways important in tumourigenesis, including signal transducer and activator of transcription 1 (STAT1) and activator protein 1 (AP1) complexes [9–11]. This action may be mediated through EBNA1 as a DNA binding transcription factor; indeed, EBNA1 binds to multiple DNA sequence sites in the cellular genome, including the promoters of genes which are transcriptionally upregulated by EBNA1, such as MEF2B, EBF1 and IL6R [12]. Recently, it has been found that EBNA1 can also influence cellular gene expression, including that of E2F1 and thence c-Myc, through a novel mechanism involving the GAr sequence of EBNA1 and the suppression of translation in *cis*. Importantly, this property is critically dependant upon the 5' sequences (hypothesised to be important in the mRNA structure) and can be abrogated by altering these sequences [5].

In view of the mounting evidence indicating an oncogenic activity of EBNA1 and the importance of this protein, both in the viral life cycle and as a therapeutic target, we sought to clarify the role of EBNA1 in lymphoma development in our transgenic mouse model of EBV-associated BL. Our data overwhelmingly point to EBNA1 as the causal oncogene in this system. We previously observed that chromosome 10, 15 and 17 amplifications were common in the EBNA1 transgenic mouse lymphomas and that the amplifications of chromosome 15 were driven by the selection for c-Myc induction [13]. We hypothesised that Mdm2 might be a candidate underlying driving force for the chromosome 10 amplifications. We now show that specific isoforms of Mdm2 are consistently overexpressed in these EBNA1-driven tumours and this is distinct from transgenic c-Myc-driven tumours. Moreover, inhibition of Mdm2 in the EμEBNA1 tumour cells leads to a dramatic down-regulation of EBNA1 and particularly E2F1 expression, accompanied by the death of the cells.

Results

Low-level expression of EBNA1 drives the tumour phenotype in EμEBNA1 line 26

Our transgenic mice were originally generated to model the viral contribution to BL, by expressing EBNA1 in B-cell cells. Two lines of EμEBNA1 transgenic mice were generated which expressed EBNA1 in the B-cell compartment (designated 26 and 59) [14]. Surprisingly, mice of line 26, which showed lower EBNA1 steady-state protein levels in pre-neoplastic lymphoid tissues compared to line 59 (despite equivalent transcript levels), displayed greater penetrance of the lymphoma phenotype [6, 14, 15].

Both transgenic lines (EμEBNA1.26 and 59) have been backcrossed into the C57Bl6/J strain for well over 70 generations and the phenotype remains unchanged, ruling out the possibility that mutations elsewhere in the genome could be responsible for the tumour phenotype. Therefore, the lymphoma phenotype maps unequivocally to the

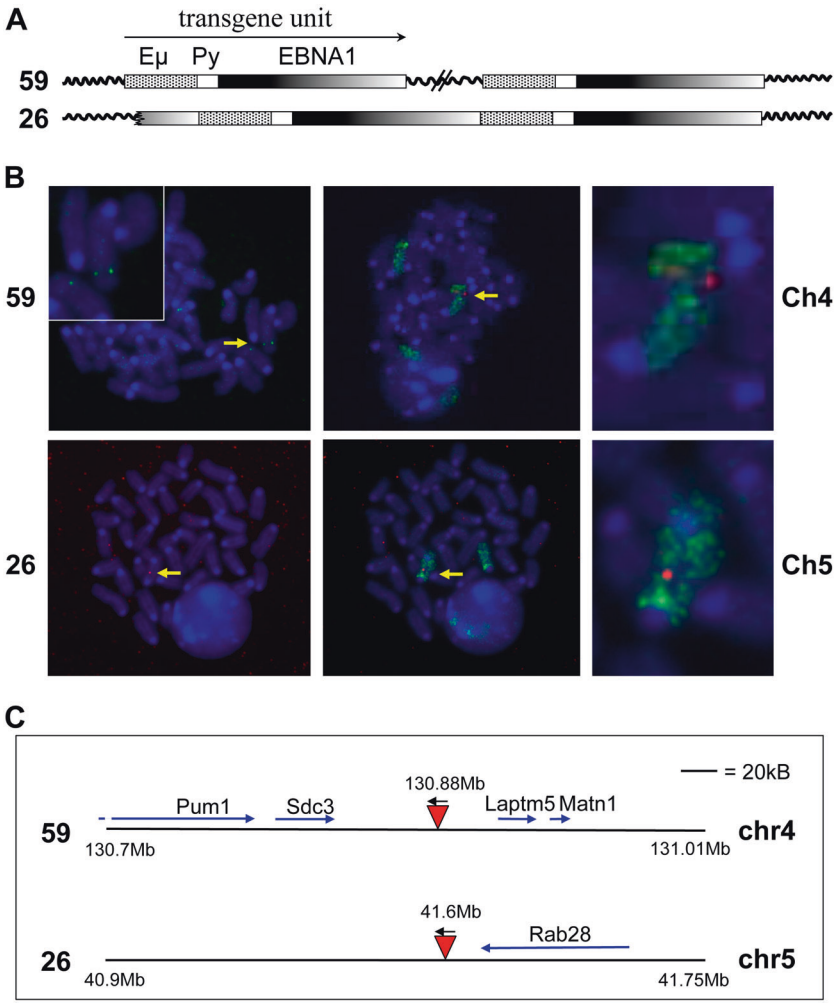

Fig. 2 The transgene integration sites. **a** The configuration of the interrupted dimeric transgene in line EμEBNA1.59 and the direct dimer in line EμEBNA1.26 are depicted. **b** FISH analysis of metaphase chromosomes from hemizygous mice of line EμEBNA1.59 (above) and line EμEBNA1.26 (below) are shown, hybridised with an EBNA1 sequence probe (arrows) and DAPI counterstained. Middle panels: whole chromosome 4 paint with line 59 samples and whole chromosome 5 paint with line 26 samples. Right panels: the transgene containing, painted chromosomes magnified. **c** Mapped location of transgene insertion sites in the two lines with respect to proximal genes (to scale as indicated)

transgene locus in each case. Crossing mice of the line 26 to other commonly used laboratory mouse strains, BalbC and FVB, revealed that the background strain can influence disease latency, but not the characteristics of the tumour or the penetrance, which remained at 100% for this line (Fig. 1a). Crossing the two lines together, to generate 2659 bitransgenic mice, showed no difference in lymphoma incidence compared to that of line 26 alone (Fig. 1b), showing that the higher expression levels of line 59 are not inhibitory to tumour development.

In order to explore if a cellular gene was disrupted or deregulated at the site of transgene insertion, the integration sites were identified. Fluorescence in situ hybridisation (FISH) of metaphase chromosomes derived from splenic cells from mice of each line, along with chromosomal painting, revealed that the transgene was integrated into chromosome 4 band D in line 59 and chromosome 5 band B in line 26 (Fig. 2). Subsequent cloning and sequencing confirmed these integration sites (detailed in SI-1, figures S1, S2 and S3). The integration site for the dimeric transgene unit of line 59 maps to mouse chromosome 4 at 130.88 Mb. This site does not lie within any known gene, the closest mapping 36 kb distal is lysosomal-associated protein (*Laptm5* at 130.91 Mb) which has no known oncogenic function (Fig. 2c). The integration site of line 26 was mapped to chromosome 5 at 41.604 Mb. There is a large gene-free region proximal to this site (3′ to the transgene unit), with heparan sulphate sulfotransferase-1 (*Hs3st1*) lying 2 Mb away at 39.6 Mb (Fig. 2c). Distal to the integration site (at 41.625 Mb) is the 3' end of the *Rab28* gene, which encodes a protein of unknown function that is postulated to be involved in intracellular trafficking (with no known oncogenic activity). The *Rab28* gene shows no rearrangements in line 26 and its expression is neither disrupted nor deregulated by the transgene (SI-1 figure S4).

Taking these data together, we have no evidence to suggest that disruption or deregulation of a cellular locus by the transgene is causal in the lymphoma phenotype of either line 26 or 59, leading to the conclusion that EBNA1 is indeed the driving oncogene in each case. Furthermore, the

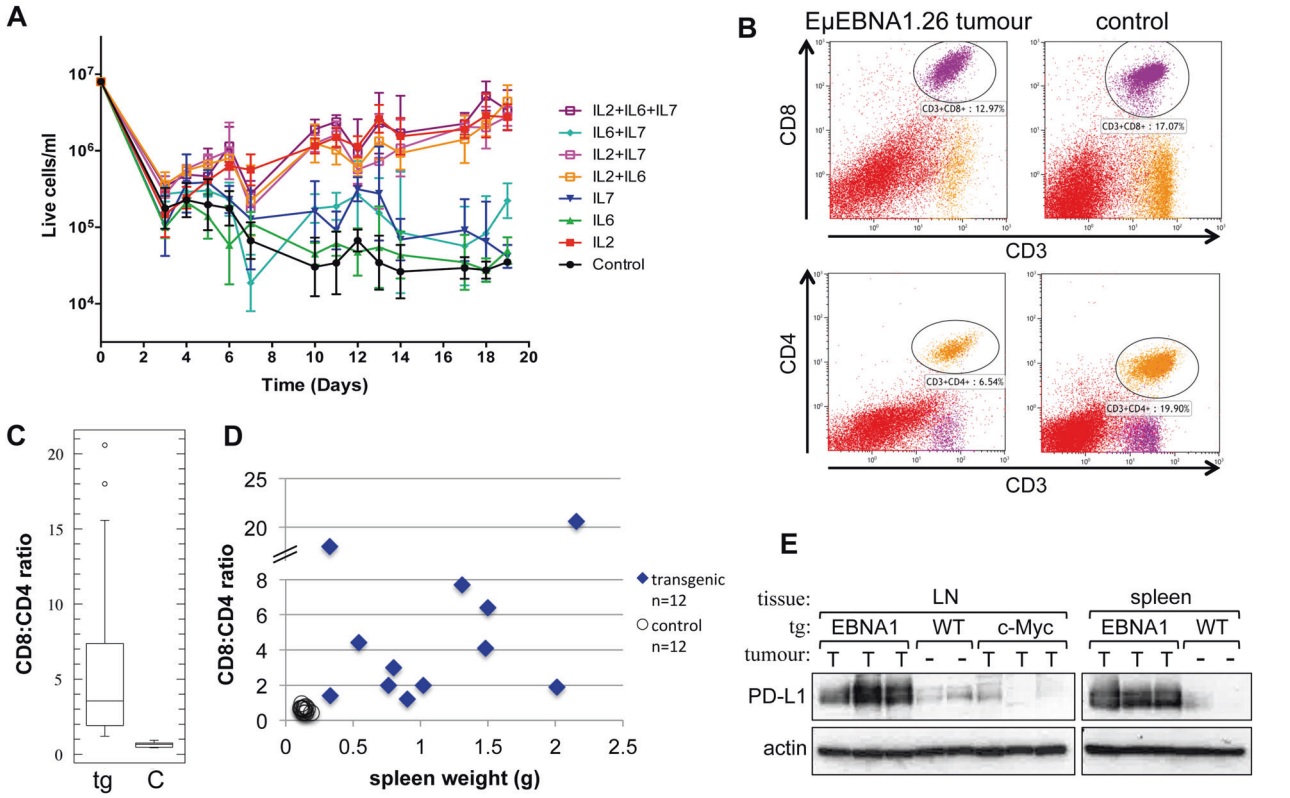

Fig. 3 T cells in the tumour environment. **a** Explanted line 26 tumour cells were cultured in triplicate, supplemented with combinations of IL-2, IL-6 and IL-7 (as indicated) or no supplement (control) and live cell numbers plotted over 20 days. **b**, **c**, **d** Explanted leukocytes from spleen tumours ($n = 12$) and aged match non-transgenic, non-tumour controls ($n = 12$) were analysed by FACS, with tumour-resident T cells co-stained for CD8, CD4 and CD3, flow histogram exemplified in (**b**). The ratio of CD8:CD4 is shown by box plot (**c**) comparing the transgenic tumour samples (tg) (mean = 6.06) and non-transgenic, non-tumour controls (C), mean = 0.64 ($p = 0.0087$) and plotted against spleen weight (**d**) which is indicative of tumour burden. **e** Expression (by western) of PD-L1 (with actin loading control below) in spleen or lymph node (LN) tumour tissues (T) from transgenic (tg) EμEBNA1.26 (26), or Eμc-Myc (c-Myc) mice, alongside non-transgenic, non-tumour control samples (−)

highly penetrant lymphoma phenotype of line 26 maps specifically to the line 26 transgene and is neither inhibited nor enhanced by higher levels of EBNA1, expressed from the line 59 transgene. Thus, it can be inferred that the pattern or nature of EBNA1 expression from the line 26 transgene is important in tumour development, consistent with the translation inhibition observed in line 26 [6].

IL-2 supports survival of the tumour cells and the tumour T-cell profile is distorted

The EBNA1 expressing transgenic B cells from both lines 26 and 59 prior to lymphoma development show prolonged survival in the presence of the T-cell cytokine interleukin-2 (IL-2) [15, 16]. Similarly, and consistent with our previous observation that the tumour B cells are CD25 (IL-2Rα) positive, addition of IL-2, and not IL-6 or IL-7, enhances the survival of the lymphoma cells in culture (Fig. 3a).

IL-2 is primarily produced by T cells and has profound and multiple effects upon both CD4 and CD8 populations [17]. Analysis at explant of the tumour-resident T cells showed that the proportion of CD8 verses CD4 T cells is significantly skewed in the tumour-bearing spleens (Fig. 3b-d), revealing an average 9.5-fold increase in the CD8:CD4 ratio. While there is a relative increase in the CD8 T-cell population within the tumour tissue, expression of the immune check-point protein PD-L1 is upregulated in the EμEBNA1.26 transgenic tumour tissue (not observed in the Eμc-Myc tumours), which would be predicted to inhibit T-cell effector functions (Fig. 3e).

EBNA1 tumour cells cannot support inhibition of EBNA1

Transfection of two B-cell lines developed from transgenic mouse lymphomas, with dominant-negative-EBNA1 (dnEBNA1) expression constructs, revealed that only the cell line which was derived from an EμEBNA1 expressing tumour was sensitive to EBNA1 inhibition (Fig. 4). The LMP1-positive mouse cell line (39.415) and the human BL

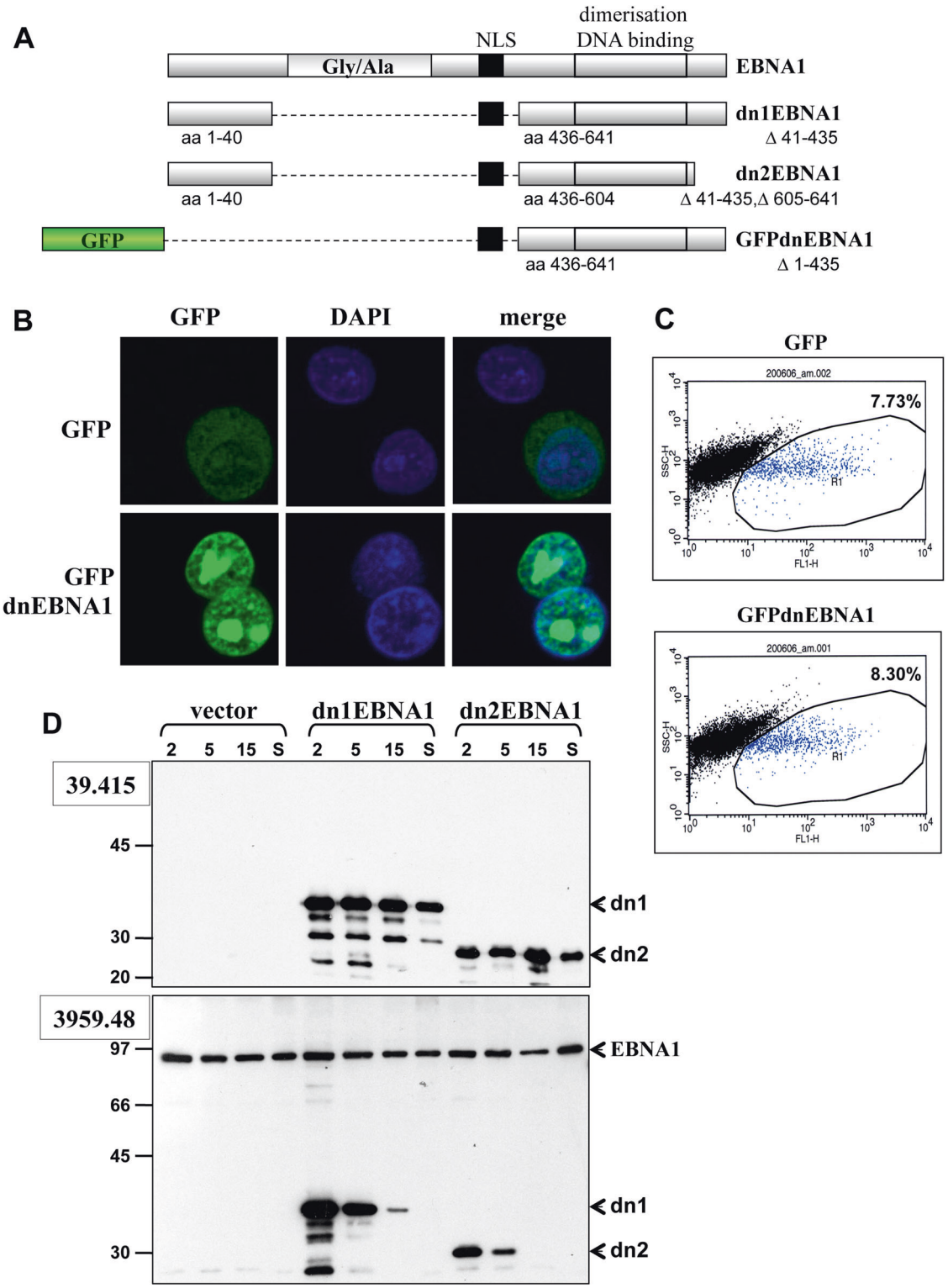

Fig. 4 Dominant negative inhibition of EBNA1. **a** The structure of 3 dominant-negative EBNA1 encoding constructs is depicted, dn1, dn2 and GFPdn-EBNA1. **b** Transfection of AK31 cells with GFPdnEBNA1 shows clear nuclear localisation (coincident with DAPI) of the dn protein, with strong nucleolar localisation. **c** Flow cytomery shows between 7 and 9% of 3959.48 cells express control GFP or GFPdnEBNA1 2 days after transfection. **d** 39.415 (LMP1) and 3959.48 cells (LMP1 and EBNA1) were transfected with empty vector or dn1EBNA1 or dn2EBNA1 constructs (as indicated). Aliquots of cells were taken for western blotting and EBNA1 detection at 2, 5 and 15 days after transfection and when stable drug-resistant cultures (S) were established (representative of 3 repeats shown). Protein size markers in kD are indicated to the left of each panel

Mouse B cells				Human B cells									
E1/no	gene ID			EBNA1/no		E1		shE1		gene			
fold	Entrez	symbol		fold	pv	1	2	1	2	Entrez	Symbol	Description
2.5	11303	Abca1	gene level	2.5	1E-04					19	ABCA1	ATP-binding cassette, sub-family A, member 1
1.9	17345	Mki67		2.1	1E-11					4288	MKI67	antigen identified by monoclonal antibody Ki-67
2.3	233016	Blvrb		1.7	0.017					645	BLVRB	biliverdin reductase B (flavin reductase)
2.4	12193	Zfp36l2		1.6	0.019					678	ZFP36L2	ZFP36 ring finger protein-like 2
2.3	58185	Rsad2		1.6	0.007					91543	RSAD2	radical S-adenosyl methionine domain containing 2
2.5	67712	Slc25a37		1.46	0.001					51312	SLC25A37	solute carrier family 25 (mitochondrial iron transporter), member 37
2.4	12349	Car2	exon level	17	5E-04					760	CA2	carbonic anhydrase II
2.3	78369	Icam4		2.1	0.022					3386	ICAM4	intercellular adhesion molecule 4 (Landsteiner-Wiener blood group)
1.8	16905	Lmna		1.9	0.041					4000	LMNA	lamin A/C
2.6	209737	Kif15		1.6	0.002					56992	KIF15	kinesin family member 15
1.9	66447	Mgst3		1.5	0.029					4259	MGST3	microsomal glutathione S-transferase 3
2.0	65246	Xpo7		1.39	0.014					23039	XPO7	exportin 7
2.0	114601	Ehbp1l1		1.37	0.025					254102	EHBP1L1	EH domain binding protein 1-like 1
-2.6	192196	Luc7l2	exon	-1.4	0.011					51631	LUC7L2	LUC7-like 2
-2.3	108155	Ogt		-1.42	0.007					8473	OGT	O-linked N-acetylglucosamine (GlcNAc) transferase
-3.2	170791	Rbm39		-1.43	0.003					9584	RBM39	RNA binding motif protein 39
-2.5	67120	Ttc14		-1.7	1E-04					151613	TTC14	tetratricopeptide repeat domain 14
-2.7	71175	Nipbl		-2.5	0.005					25836	NIPBL	Nipped-B homolog
-2.4	76499	Clasp2		-3.7	0.04					23122	CLASP2	cytoplasmic linker associated protein 2
-1.9	241915	Phc3	gene	-1.32	0.039					80012	PHC3	polyhomeotic homolog 3
-2.2	108655	Foxp1		-2.3	0.006					27086	FOXP1	forkhead box P1

Fig. 5 Genes deregulated by EBNA1 in common to mouse and human samples. Genes showing the same direction of deregulation in the presence (red in heat map) or absence (blue inheat map) of EBNA1 are listed, giving the fold change, mouse and human gene symbols and Entrez ID

cell line AK31 could support persistent expression of dnEBNA1 throughout selection and stable dnEBNA1-expressing cell lines were established (Fig. 4). By contrast, with the LMP1+/EBNA1+cell line (3959.48), dnEBNA1 expression was detected 2 days after transfection (Fig. 4c, d), was considerably reduced by 5 days and lost by 2 weeks of selection. All cultures and clones established following selection and stable retention of the G418-resistance encoding plasmid in this cell line did not express dnEBNA1. This suggests that expression of dnEBNA1 is not compatible with the outgrowth of this LMP1/EBNA1-positive transgenic lymphoma cell line, which in turn indicates that EBNA1 provides a selectable growth advantage to the cells that can be inhibited by the dnEBNA1 proteins.

Cellular genes deregulated by EBNA1

EBNA1 is known to function as a transcriptional regulator and bind to cellular chromatin. In order to determine if EBNA1 deregulates the transcription of cellular genes in the line 26 transgenic model, a global analysis of expressional changes was conducted using microarrays. Splenic B cells from young mice were selected, at an age when the transgenic mice are phenotypically normal, with no evidence of lymphoma. This was chosen in order to specifically examine EBNA1-driven predisposition and to preclude the detection of expressional changes induced by mutations that occur through tumourigenesis. Complementary DNA (cDNA) samples from 5 transgenics and 5 non-transgenic sibling controls (NSC) were compared. Modest expression differences were observed: 89 genes showed a significant upregulation in the presence of EBNA1 and 46 significant downregulation with a maximal difference of 4.45-fold (SI-2). Several of the identified genes have been previously published as targets of EBNA1-mediated deregulation, including Stat1, Id2 and AP1 family members (with c-Fos, FosB, JunB identified here) [9, 11].

To further explore any similarity between mouse and human cell responses to EBNA1, we compared this mouse gene set with a published set of genes identified as showing expressional changes at the RNA level (by RNA sequencing (RNA-seq)), following small hairpin RNA (shRNA) inhibition of EBNA1 expression in a human Mutu-EBV-positive lymphoblastoid cell line (LCL) [12]. Of the 135 listed mouse genes (SI-2), a matched human homologue was identified for 114. Of these, 21 showed significant changes at the gene or exon level in the human RNA-seq data, with the same fold direction between EBNA1 present or absent (Fig. 5). Interestingly, one of these genes (Slc25a37, encoding a mitochondrial iron importer) also shows an EBNA1 binding site within 10 kb from the transcriptional start site [12]. As well as a notable preponderance of genes with a metabolic role in the common set, the marker of proliferation, Ki-67 is upregulated by EBNA1.

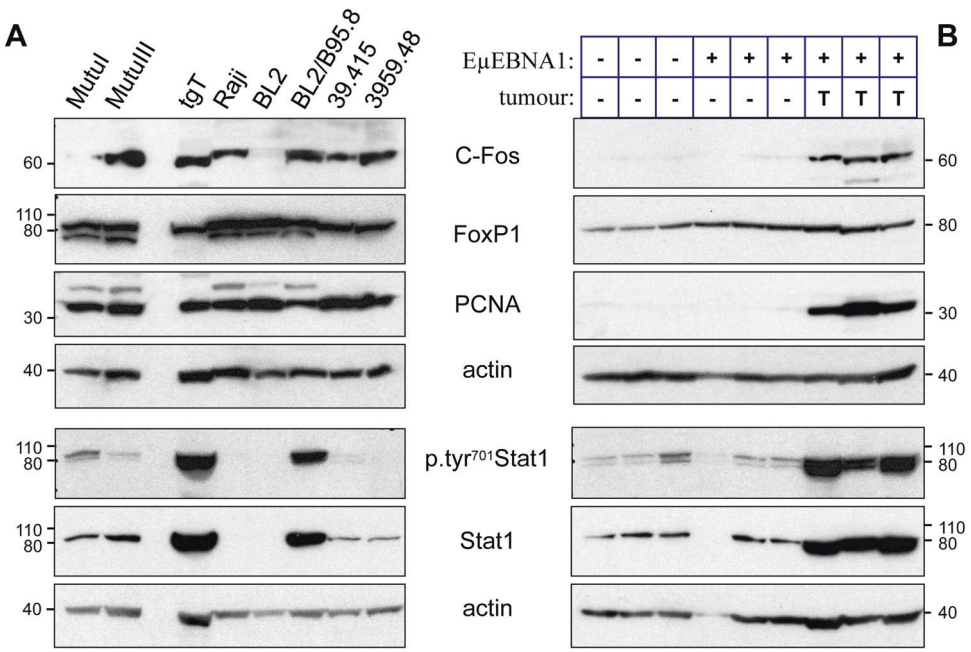

Fig. 6 A selected comparison between mouse and human samples. Protein extracts were examined in human and mouse cell lines (**a**) and from mouse lymph node tissue (**b**), by western blotting for the expression of c-Fos, FoxP1, PCNA, Stat1 and phosphor-tyr-701 Stat1, using actin as a loading control (as indicated). In (**a**) tgT is an EμEBNA1 transgenic mouse lymph node tumour sample. In (**b**) EBNA1 transgenic status is indicated (−/+) and no-pathology or tumour (−, T respectively) above each track. Note that the FoxP1 antibody recognises a doublet in human samples, with a single band in mouse samples; the PCNA antibody also recognises a larger band (~35 kD) in human samples; the p.tyr701-Stat1 antibody recognises a doublet in both species, the upper band of which (~90 kD) is recognised by the antibody to total Stat1. Protein size markers in kD are indicated to the side of each panel

Selected genes from the mouse list (SI-2) were examined for expression at the protein level in both human and mouse cell lines, as well as transgenic and control mouse tissue (Fig. 6). C-Fos (one of two genes showing over fourfold RNA upregulation in the presence of EBNA1) is expressed in both mouse B-cell lines examined and in the EBV-positive human BL cell lines MutuI, MutuIII and Raji (at lower levels in MutuI), but is absent from the EBV-negative cell line BL2. Interestingly, in the EBV converted BL2/B95.8 cell line c-Fos expression is induced compared to the parental BL2. C-Fos is upregulated in the EBNA1 transgenic mouse tumour tissue while it is barely detectable in the normal lymph node tissues of NSC mice and pre-tumour, young EBNA1 transgenic mice. Similarly, Stat1 and its tyr701 phosphorylated form (allowing dimerisation and nuclear entry) are upregulated in the EBNA1 transgenic mouse tumour tissues compared to normal tissue, and BL2/B95.8 compared to BL2 (the latter shows no expression). Stat1 is expressed and tyr701 phosphorylated in the Mutu cell lines. Proliferating cell nuclear antigen (PCNA), like Ki67 is a proliferation marker and is strongly expressed in all the cell lines examined and the transgenic EBNA1 tumours, with very low detection in the tissues of normal pathology. Contrary to the RNA data, FoxP1 was readily detectable in all samples (cell lines and tissues), with possibly slightly higher levels in the EBNA1 transgenic tissues compared to NSC.

EBNA1-driven tumours show upregulation of specific Mdm2 isoforms

Prior to tumour development, the expression level of EBNA1 is very low in the line 26 B cells, but this substantially increases upon tumour development [14]. Similarly, the expression levels of both c-Myc and E2F1 are highly induced in the EBNA1 transgenic lymphomas (Fig. 7). P53 is expressed at high levels in the EμEBNA1.26 tumour tissues, as well as tumours arising in Eμc-Myc mice and bitransgenic mice. The high levels of p53 in these tumour tissues suggest that it could be mutant, and indeed in some samples, p53 migrates at different sizes (Fig. 7). The chromatin remodelling factor, metastatic tumour protein-1 (Mta1), a master co-regulator of oncogenes, can act to inhibit p53 ubiquitination and thereby contribute to its stabilisation [18]. Interestingly, it is also induced in all of the EμEBNA1 tumours, but in only 1 out of 3 of the Eμc-Myc tumours. Translation of the anti-apoptotic protein Xiap is promoted by Mdm2, through its C-terminal RING domain and this protein was also found to be upregulated in the EBNA1 tumours (Fig. 7).

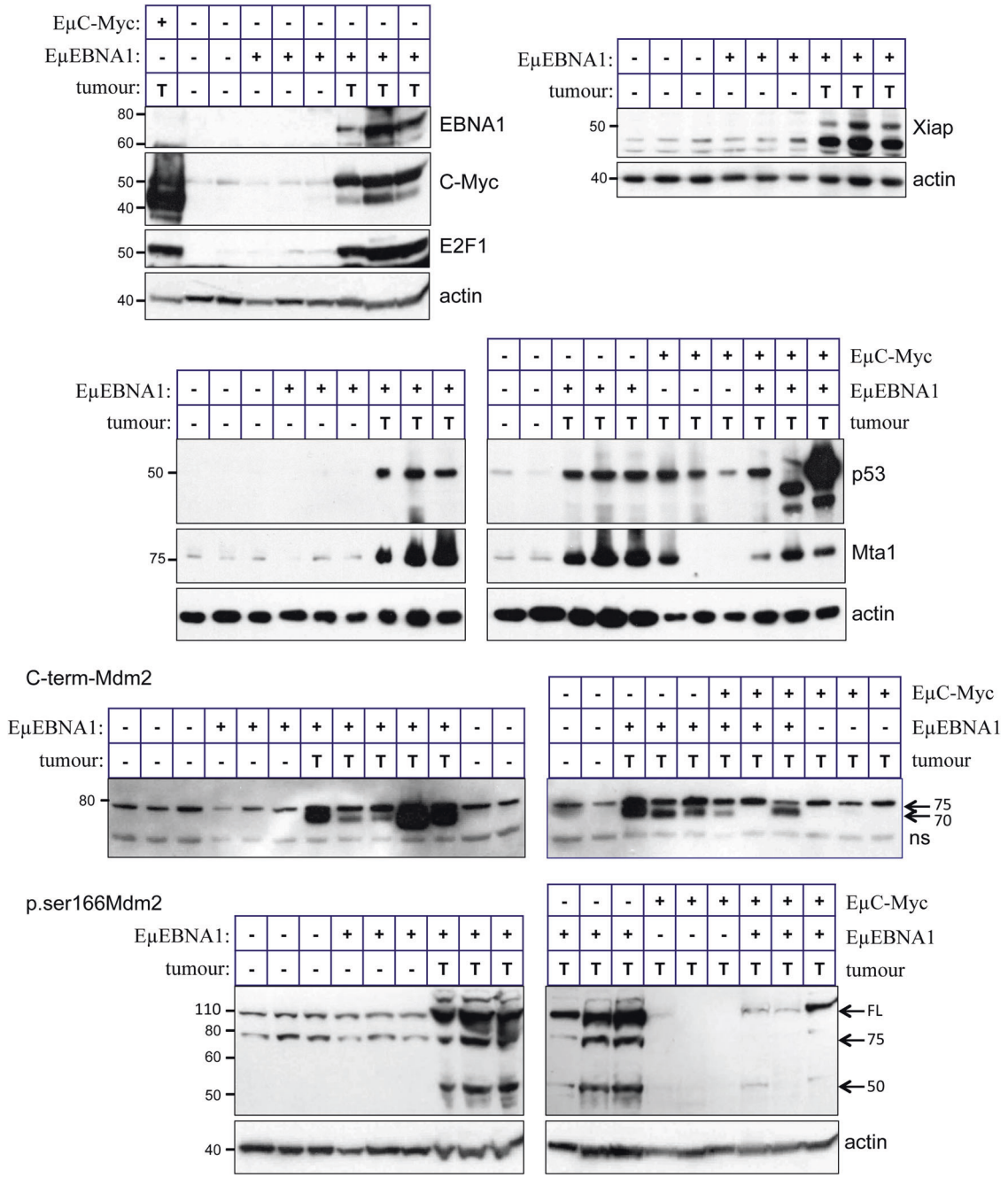

Fig. 7 Proteins deregulated in EBNA1 transgenic tumours. Heavily tumour invaded lymph node samples (T), or non-tumour controls (tumour −) were analysed by western blotting for the expression of EBNA1, c-Myc, E2F1, p53, Xiap, MTA1 and Mdm2, using actin as a loading control, or non-specific binding (ns) as loading indicator. For Mdm2, antibodies recognising either phosph-ser166 or a C-terminal region were used (p.ser166Mdm2 and C-term-Mdm2 respectively). Mdm2 isoforms are indicated by size, or full length (FL, migrating at approximately 90 kD). Each sample represents a distinct primary tumour (tissue taken from different mice). Samples were from mice transgenic for EμEBNA1 (line 26), Eμc-Myc, bitransgenic for both or NSC (−), as indicated. Samples were also taken from EμEBNA1.26 at 2 months of age from normal phenotype lymph nodes prior to development of tumour (indicated as EμEBNA1 +, tumour −). Note that in these pre-tumour transgenic samples, EBNA1 expression is below detection at these blot exposures. Protein size markers in kD are indicated to the left of each panel

The *Mdm2* gene produces numerous differentially spliced transcripts, encoding multiple isoforms of the protein, which have different functions [19–21]. Using antibodies against different epitopes, including phosphorylated ser166, we found that several isoforms of Mdm2 are upregulated in the EBNA1 tumours. The major forms detected include: full-length Mdm2 (FL-Mdm2) phosphorylated on ser166, a 75 kD ser166-phosphorylated

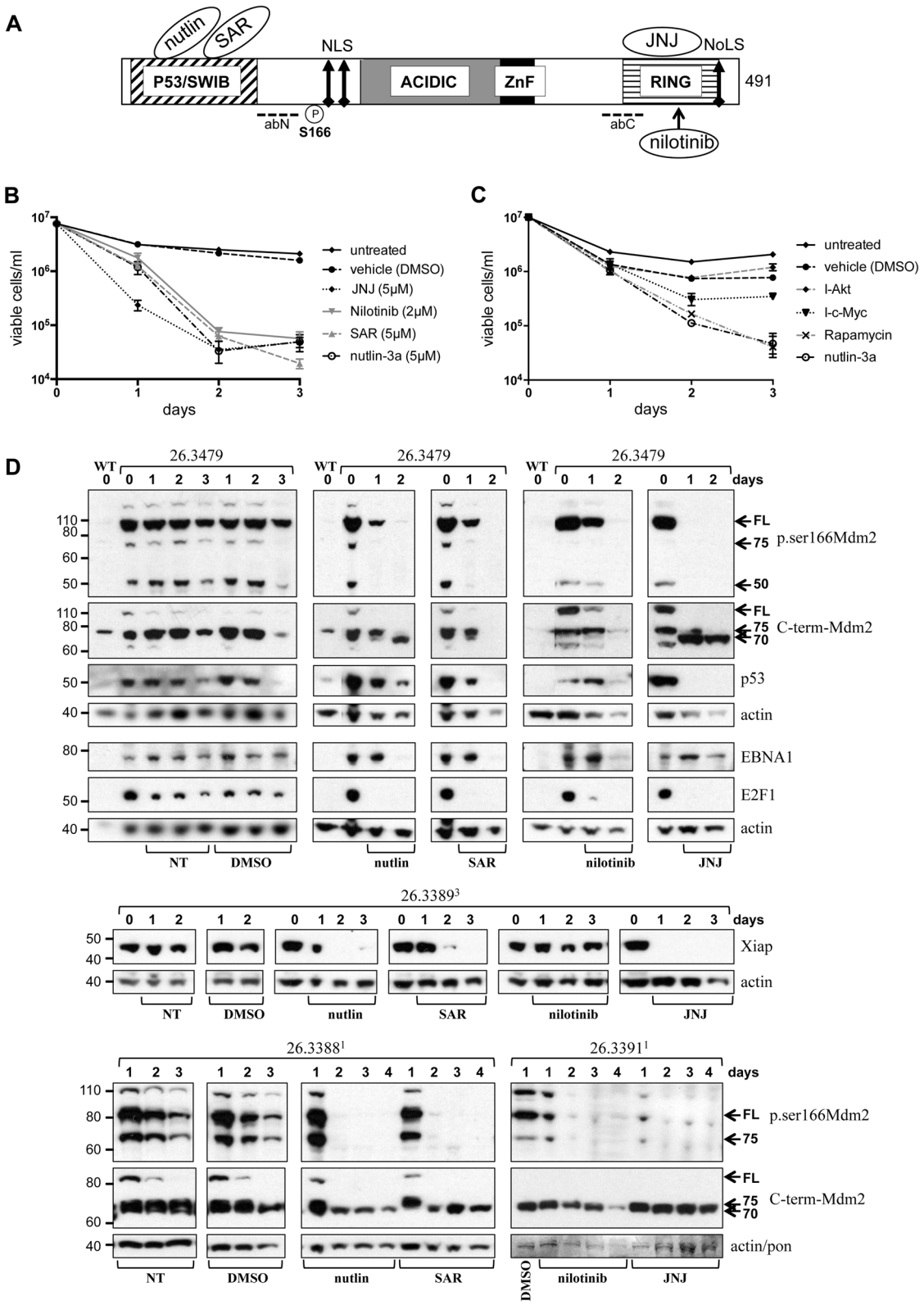

isoform, an N-terminal 50 kD ser166-phosphorylated isoform and a tumour-specific highly abundant 70 kD isoform (Fig. 7). A phospho-band detected at ~160 kD may reflect a multimer. The 70 kD isoform could not be detected by the N-terminal-directed antibody or the phospho-ser166 antibody and likely represents a form which is deleted for N-

◀ **Fig. 8** Mdm2 inhibitors kill the EBNA1 tumour cells. **a** Diagramatic representation of the domains of Mdm2 in linear form, showing the p53 binding region, acidic domain, Zn-finger motif and ring domain. Approximate action sites for the inhibitors are shown, with nutlin-3a and SAR405838 (SAR) competing with p53 binding, and JNJ26854165 (JNJ) and nilotinib acting at the C-terminal region. Epitopes for the antibodies used in these studies are depicted with dashed lines: abN: N-terminal epitope, abC: C-terminal epitope and to phosphor-serine166 (S166). The nuclear localisation signals (NLS) and nucleolar localisation signal (NoLS) are shown (arrows). **b** Primary EμEBNA1.26 tumour cells were treated with each Mdm2 inhibitor (as indicated) at 5 μM (2 μM for nilotinib), compared to untreated or vehicle only (DMSO) and live cell numbers measured for 3 days (triplicate experimental replicates). Error bars = SD. **c** Primary EμEBNA1.26 tumour cells were treated with Nutlin-3a, rapamycin and inhibitors of c-Myc and Akt (I-c-Myc and I-Akt respectively), all at 5 μM, compared to untreated or vehicle only (DMSO) and live cell numbers measured for 3 days (in triplicate) Error bars = SD. **d** Protein extracts from Mdm2 inhibitor-treated tumour cells collected after up to 4 days of treatment, compared to untreated cells and non-transgenic leukocytes (WT), were western blotted, using antibodies as indicated. Representative samples from cells from four different tumours are shown (ID: 26.3479, 26.3389, 26.3388, 26.3391 where superscript indicates in vivo passage number of the tumour). Protein size markers in kD are indicated to the left of each panel

terminal exons. This isoform is consistent with the Mdm2A or Mdm2C splice variant products, which lack exons 4 to 9 (amino acids 28 to 222) or 5 to 9 (amino acids 53 to 222) (respectively) and migrate at approximately this size [19, 22]. The 75 kD isoform is phosphorylated on Ser166 and therefore must be encoded by a transcript that includes exon 8. Of note, in B-cell lymphomas which arise in Eμc-Myc mice, the 70 kD form is not expressed, with little or no detection of phospho-50 kD, phospho-75 kD and phospho-FL-Mdm2. Only the ser166-unphosphorylated 75 kD isoform was readily detected in Eμc-Myc tumours, similar to non-transgenic controls. Bitransgenic tumours, expressing both c-Myc and EBNA1, showed a mixed profile (with 50% showing the Mdm2 induction), which may reflect the degree of functional involvement of EBNA1 in the development of each tumour. We have examined over 20 independent tumours from the EμEBNA1.26 line and all show this Mdm2 upregulation profile. No Eμc-Myc tumours (over 10 independent tumours examined) display this Mdm2 activation pattern. Therefore, the increased phosphorylation of the 50 kD, 75 kD and FL isoforms and the upregulation of the 70 kD isoform are specific to the EBNA1-driven tumours. It follows that this specific Mdm2 isoform expression and activation pattern is factorial in EBNA1-driven tumourigenesis.

Inhibition of Mdm2 kills the EBNA1-driven tumour cells and leads to loss of E2F1

In order to examine the dependency of the transgenic mouse EμEBNA1 tumour cells upon Mdm2, we treated cells with Mdm2 inhibitors. Nutlin-3a and SAR405838 bind to Mdm2 within the p53-binding pockets (thus competing with p53 binding), leading to p53 stability by inhibiting its ubiquitin-mediated degradation [23, 24]. Nilotinib was developed as an inhibitor of c-Abl kinase (for which Mdm2 is a substrate) and this compound causes disruption of the Mdm2/Mdmx heterodimer (involving the C-terminal region) and consequent destabilisation of Mdm2, and inhibition of the translational promoting activity of Mdm2 upon *Xiap* mRNA [25, 26]. The small molecule JNJ-26854165 binds to the C-terminal RING domain of Mdm2 and inhibits its ubiquitin ligase activity [27]. Primary tumour cells isolated from EμEBNA1.26 transgenic lymphomas were cultured in each drug, with the experiment repeated at least four times using different primary tumours (Fig. 8). All four Mdm2 inhibitors led to a significant decrease in EμEBNA1 tumour cell viability compared to vehicle-only treated controls, with almost complete cell death by 4 days of treatment. In contrast, transgenic Eμc-Myc primary lymphoma cells showed no loss of viability with treatment at the same concentration and while primary normal leukocytes showed some sensitivity, cultures were still viable after 3 days of treatment (SI-1 Fig S5 and S6). With the EμEBNA1 tumour cells, all four drugs resulted in loss of FL-Mdm2, the 75 kD and 50 kD ser166 phosphorylated isoforms by day 2, and with JNJ, by day 1. Interestingly, the abundant (non-phosphorylated) 70 kD isoform was more stable. Also, the non-phosphorylated 75 kD isoform was lost by day 2 with nutlin-3a and SAR treatment, but appeared to be stable with nilotinib and JNJ treatment, and thus the drugs show differential effect with respect to particular isoforms. While p53 remained stable with nutlin-3a treatment, p53 could not be detected after 1 day of treatment with JNJ. Similarly, Xiap was undetectable by 1 day of treatment with JNJ, by day 2 with nutlin-3a and SAR treatment, but remained detectable over 3 days with nilotinib treatment. EBNA1 levels were reduced by day 2 with all four drugs. However, the most profound effect of Mdm2 inhibition was upon E2F1 which was completely lost by day 1 with all four drugs.

To examine the potency of Mdm2 inhibitors upon the EBNA1 tumour cells in comparison to other key drug targets, primary tumour cells were treated with inhibitors of c-Myc, Akt and mTor (10058-F5, Akt-inhibitor II and rapamycin, respectively). At recommended doses, the c-Myc inhibitor and nutlin-3a led to rapid death of the cells, while rapamycin and the Akt inhibitor had little effect (SI-1 Fig S7). At equimolar doses, the increase in rapamycin dose showed effective cell killing (as might be expected of this translational suppressor) and the reduced dose of the c-Myc inhibitor showed a reduction in killing efficacy while the Akt inhibitor remained ineffectual (Fig. 8c).

Human BL cell lines express several isoforms of the Mdm2 orthologue (Hdm2) and little difference was detected

between EBV-positive and -negative or the Mutu cell lines in latency I and III (SI Fig S8). However, treatment of these cell lines with the Mdm2 inhibitors JNJ and nultiln-3a over 3 days revealed a difference between EBV in latency I and III, consistent with earlier data conducted over 24 h [28]. Raji cells (EBV latency III), BL2/B95.8 (transformed with EBV in latency III) and Mutu III (EBV latency III) all showed reduced sensitivity to both drugs compared to BL2 (EBV negative) and MutuI (EBV latency I) (SI Fig S9). Notably, MutuI cells were largely dead after 3 days culture with both inhibitors, while MutuIII showed growth inhibition, but not loss of viability.

Discussion

There is a correlation between EBNA1 translation suppression and EBNA1-associated tumourigenesis. Mice of the two EBNA1-expressing transgenic lines (EμEBNA1 lines 26 and 59) develop B-cell lymphoma, but with significantly greater incidence in line 26 [6]. We previously showed that while EBNA1 transcript levels in lymphoid tissues were similar between the two lines, EBNA1 protein levels in line 26 before tumour development were far lower than line 59, suggesting that the transgene of line 26 is subject to translation suppression. We further showed that the transcripts differed between the two lines in the utilisation of 5' start sites, with line 26 showing more initiation upstream of the canonical promoter [6]. In addition, 3 lines of EBNA1 transgenic mice developed by Kang et al. [29], using a different transgene promoter and incorporating a 5' in-frame FLAG-tag, showed high levels of EBNA1 expression and no tumour phenotype. Recent studies have now provided a solution to the puzzling relationship between EBNA1 translation suppression and tumour development. The mechanism of in-*cis* translation inhibition, mediated by the GAr of EBNA1 (and critically dependant upon the configuration of 5'sequences), leads to an mRNA translation stress response resulting in an increase in E2F1 synthesis and the consequent induction of c-Myc expression, thereby contributing to cell proliferation [5]. As such, this predicts a direct correlation between EBNA1 translation suppression and tumourigenicity by EBNA1, which would be observed as an inverse correlation between EBNA1 protein levels (presumably above a basal minimum) and its oncogenic action. This is indeed what is observed experimentally, with the line showing highest tumour penetrance (line 26) showing low levels of EBNA1 prior to tumour development, and high EBNA1 expressing mouse lines showing no tumour phenotype [29].

Prior to the development of tumours, in EμEBNA1.26 B-cells, we observed changes in transcript levels of numerous genes, several of which have been previously shown to be deregulated by EBNA1 in human cells [9, 11]. Amongst these, C-Fos and Stat1 were also shown to be upregulated at the protein level in the transgenic mouse tumours and induced in the EBV-converted BL2/B95.8 cell line, compared to the parental, EBV-negative BL2 cell line, which shows no expression. Additionally, parallels could be drawn in a direct comparison of gene sets identified with respect to one variable, that of EBNA1 expression, but derived from two very different cells systems: the mouse pre-tumour EBNA1 deregulated transcripts, and those showing difference after EBNA1-RNA interference of an LCL [12]. However, while FoxP1 (a tumour suppressor) showed lower transcript levels with EBNA1 presence in both systems, this was not recapitulated at the protein level, which may reflect a functioning autoregulatory process.

High-level expression of EBNA1 has been found to inhibit the growth of EBV-negative BL cell lines [7]. However, the higher levels of EBNA1 expression driven from the line 59 transgene was not inhibitory to the tumour development observed in line 26 (as observed in the 26/59 bitransgenic study). Importantly, investigation of the transgene insertion sites has yielded no evidence that cellular genes at these sites contribute to, or inhibit, the tumour phenotype, leading to the conclusion that EBNA1 and its pattern of expression in the transgenic mouse line 26 is the driving oncogenic force.

Together, these data suggest that EBNA1 is acting as an oncogene through several routes in the transgenic mice. Firstly, the mechanism of expression is important, with GAr translation suppression being a key contributing factor in the high tumour incidence of line 26. Secondly, EBNA1 protein–protein interactions are likely to play a role, as Mdm2 (a substrate for the EBNA1 binding protein USP7) is critical in the tumourigenic process. Thirdly, EBNA1 has an impact upon the expression of cellular genes at the RNA level. This may be achieved through the action of EBNA1 as a transcriptional regulator, and/or as a result of the first two mechanisms. One consequence of the tumour cell expression profile points to T-cell support of the tumours through IL-2, while the induction of PD-L1 suggests that the immune response is compromised [30].

The consistent and dramatic increase in EBNA1 protein levels from pre-tumour tissue to tumour indicates that this is a positive selection force in tumourigenesis. That at least part of the oncogenic activity is independent of the translation mechanism and instead is due to EBNA1 protein action is supported by the observation that dominant negative inhibitors of EBNA1 (proposed to block EBNA1 function) inhibit the growth of an EμEBNA1 lymphoma-derived mouse cell line.

C-Myc upregulation is inextricably associated with the EBNA1-mediated tumourigenic process and we previously showed that this is achieved, at least in part, by mutation.

The line 26 tumours commonly harbour trisomy 15 (the location of mouse c-Myc), which was completely absent in mice bitransgenic for EμEBNA1 and Eμc-myc as these overexpress c-Myc from the outset. Similarly, the *c-myc* locus was identified as a common insertion site of MoMLV, using the provirus as a mutagenic cooperative gene tag in tumourigenesis in the EμEBNA1 mice [13]. Accordingly, small molecule inhibition of c-Myc leads to the death of these EμEBNA1 tumour cells. This is consistent with BL, in which translocation of the c-Myc locus and deregulation of c-Myc expression is a characteristic.

We now show that deregulation of Mdm2 is a critical event in the process of EBNA1-mediated tumourigenesis and that specific isoforms are induced and phosphorylated at ser166, including full-length, 75 kD, 50 kD and a ser166-non-phosphorylated 70 kD C-terminal isoform. As Mdm2 is not apparently overexpressed prior to the onset of tumourigenesis, but is highly upregulated in every EBNA1 tumour, this is likely to be driven by epigenetic changes or mutation and growth advantage selection. Importantly, the levels of expression of Mdm2 and EBNA1 are linked. Inhibition of Mdm2 leads to loss of Mdm2 and loss of EBNA1 expression. As well as the complex, mutually regulative functions between Mdm2 and p53, Mdm2 facilitates Xiap translation via the C-terminal ring domain [27] and can also act as a chaperone to assist in the protein folding of p53 [19]; additionally, it plays a role in nucleolar stress responses [31]. Thus, Mdm2 may facilitate EBNA1 translation and/or protein folding. In support of this hypothesis, the most highly upregulated isoform of Mdm2 in the EBNA1 tumours (70 kD) lacks part of the N-terminal region, retains the C-terminal region and is consistent with the human splice variant Mdm2A which encodes a p53-independant oncogenic form of Mdm2 [19]. Inhibition of Mdm2 in the EBNA1 tumour cells also led to the loss of all ser166 phosphorylated species of Mdm2 (FL, 75 kD and 50 kD and multimers). This site is phosphorylated by Akt and enables Mdm2 nuclear localisation and stability. It is not known exactly how the inhibitors act, but all four resulted in loss of the ser166-phosphorylated species, the C-terminal binding compound JNJ-26854165 being the most potent.

The cell cycle regulator E2F1 is abundantly overexpressed in all the EBNA1 tumours and inhibition of Mdm2 led to rapid loss of E2F1. Mdm2 interacts through both its N-terminal region and the RING domain with E2F1 [19] and is able to stabilise E2F1 thereby promoting cell proliferation [32]. However, in p53 wild-type cells, E2F1 inhibits Mdm2 expression at the promoter, which does not occur in p53 mutant cells [33].

This leads to our working hypothesis that in the genesis of these EBNA1 tumours, overexpression of Mdm2 enhances both EBNA1 and E2F1 protein expression and stability. The E2F1 transactivation function (upon *c-Myc* and other cell cycle regulators), in conjunction with the deregulation of the *c-Myc* gene by mutation, promotes proliferation. Mutation of p53 would facilitate this process by breaking the feedback loop of E2F1 inhibition upon Mdm2 expression and indeed, C-terminal isoforms of Mdm2 (such as the human Mdm2A, B and C isoforms which do not have the p53 binding domain) have been shown to promote expression of mutant p53 and its gain of function action in tumourigenesis [21, 34]. Many other players are clearly involved in the genesis of these EBNA1-driven tumours, such as Xiap, which acts to inhibit apoptosis and Mta1, a master co-regulator of gene expression and inhibitor of ubiquitination and degradation of p53 [18].

In human BL, all tumours harbour a rearranged c-Myc gene with deregulated expression. Similarly, most BL tumours have mutant p53 and EBV latency I BL cell lines express Mdm2 and are sensitive to Mdm2 inhibition [28]. Therefore, our transgenic EμEBNA1 tumour model shares several key features with EBV-positive BL. In culture, EBV-positive BL cells tend to drift to a latency III state, with the induction of the other viral latent genes. This is likely to have a significant impact on the tumorigenic environment, exemplified by the action of EBNA2 upon *c-Myc* [35] and the cells lose sensitivity to Mdm2 inhibition.

In conclusion, we have shown that EBNA1 is a driving force in the transgenic mouse tumours and provides a relevant model for EBV-associated BL, both for investigation and testing therapeutic treatment strategies. Deregulation of key cellular genes are required during the EBNA1-driven tumourigenic process; as well as c-Myc, Mdm2 induction is pivotal. Identification of the latter provides new insight into the role and function of EBNA1 in tumourigenesis and the viral life cycle and opens therapeutic routes for the treatment of EBV-associated disease.

Materials and methods

Mouse microarray data and comparison with human Mutu-LCL RNA-seq data

RNA was prepared from B cells, selected from spleens of 2-month-old mice (which show no pathology), using mouse panB (B220) Dynabeads [15]. Five EμEBNA1.26 and 5 negative sibling controls (NSC) were used. RNA was polyA selected and cDNA used as a probe on Affymetrix arrays (murine genome U74v2:A, B, C). Genes showing RNA levels with a statistically significant difference between transgenic and NSC and with a false error rate below 0.05 are listed (SI-2 table S4).

Information was obtained from the MGI-Mouse vertebrate homology database to identify the human homologues of the listed mouse genes. Of these, 114 showed matched

unique human homologues (74 upregulated in the presence of EBNA1 and 40 downregulated). Of these, 21 genes showed matched changes in the mouse data set with the published Mutu-LCL shRNA data set [12] (13 upregulated in the presence of EBNA1 and 8 downregulated), with a trend in significance of overlap measured by hypergeometric test ($p = 0.053$ and 0.071 respectively).

Transgenic mice and screening

The two transgenic mouse lines, EμEBNA1.26 (line 26) and EμEBNA1.59 (line 59), encoding EBNA1 of the B95-8 strain, have been previously described [6]. Non-transgenic sibling controls (NSC) are used in these studies. Mice were maintained under conventional housing conditions. All procedures have been conducted under Home Office licence and the research complied with and was approved by Home Office and institutional guidelines, ethical review and policies. Tail genomic DNA was prepared [36] and screened by PCR for transgenic status using B and R oligos (SI-1 table 3). Samples were also used from mouse lines Eμc-Myc and EμBcl2, described previously [13, 16].

Western blotting

Proteins were extracted in RIPA buffer and separated (10–50 μg per track) by sodium dodecyl sulfate–polyacrylamide gel electrophoresis (7.5%, 10% or 4–12% gradient NuPage (Invitrogen)); blotting, blocking, washing and detection were performed essentially as previously described [15]. Antibodies used are listed in SI-1 table S1. At least three experimental replicates (tissues from different mice) were used to analyse transgenic and NSC samples.

Cell culture and treatments

Cells were cultured in RPMI-1640 medium supplemented with 10% fetal bovine serum (FBS), 2 mM L-glutamine, 100 U/ml penicillin, 100 μg/ml streptomycin, with 50 μM 2ME for primary cells. Human BL cell lines used include: BL2, BL2/B95-8, AK31 (EBV-negative derivative of Akata), Raji, MutuI and MutuIII. Mouse lymphoma B-cell lines derived from transgenic tumours are: 39.415 (LMP1 positive) and 3959.48 (LMP1 and EBNA1 positive) [37]. Cells were transfected by electroporation, and selected by G418 supplement, as previously detailed [37]. Primary lymphoma cells explanted from the EμEBNA1.26 line (each tumour from independent mice carry unique I.D. numbers), or in vivo passages of these tumours (through C57Bl/6J recipient mice, superscript denoting passage number where relevant), or wild type (NSC) splenocytes, were explanted, red blood cells lysed (in 0.75% NH_4Cl, 0.017 M Tris pH 7.2), and the leukocytes washed several times in phosphate-buffered saline (PBS) and either cultured directly, frozen (90% FBS, 10% dimethyl sulfoxide (DMSO)) for subsequent culture or analysed by fluorescence-activated cell sorting (FACS). Cell culture supplements were IL-2 (16 ng/ml), IL-6 (1 ng/ml) and IL-7 (16 ng/ml). Drug treatment of cells was by daily addition of Nutlin-3a, SAR-405838, JNJ-26854165, Nilotinib, C-Myc inhibitor 10058-F4, Akt inhibitor and Rapamycin (SI-1, table S2), dissolved at 100× or 1000× in DMSO), for up to 4 days. Live cell counts and viability were determined by Trypan blue exclusion using the Countess Automated Cell Counter (Thermo Fisher Scientific).

Flow cytometry

Isolated leukocytes (from tumour-bearing spleens or controls) were washed in PBS, 1% FBS and strained (30 μM filter). Cells were preincubated with Trustain (10 min, ice) and 10^6 aliquots used for FACS, staining with conjugated antibodies against surface markers: CD3-APC, CD4-FITC, CD8-PE and CD19-PE (Ebiosciences). Cells were analysed using a CyAn ADP Analyser (Beckman Coulter) and Kaluza software.

Fluorescence in situ hybridisation

Explanted splenocytes were washed, and incubated in medium with lipopolysaccharide (50 μg/ml) for 45 h at 37 °C. Cells were then treated with colcemid (10 μg/ml) for 1 h, hypotonically shocked by resuspension in 75 mM KCl, collected and fixed in methanol/acetic acid (3:1), applied to slides and air dried. A SpectrumGreen or SpectrumRed (Vysis) labelled EBNA1 3' sequence probe (*Bst*XI-*Eco*RI 1 kb transgene fragment) was hybridised, with or without chromosome 4 and 5 paint probes (Cambio), to denatured chromosomes, essentially as previously described [38, 39]. Samples were counterstained with 0.5 μg/ml 4',6-diamidino-2-phenylindole (DAPI) in Vectashiled (Vector) and examined using a Zeiss Axioplan fluorescent microscope.

Cloning, sequences and plasmids

Transgene integration sites were cloned by inverse PCR and phage λ library screening (detailed in SI-1). The dominant-negative EBNA1 encoding constructs (generated in pcDNA3.1myc-His at *Bam*HI and *Xba*I sites incorporating in-frame C-terminal myc and His tags) are deleted between the natural EBNA1 *Nco*I and *Apa*I sites (amino acids 41 to 435 of EBNA1) with the EBNA1 nuclear localisation signal re-inserted at this site (SI-1 table S3). GFPdnEBNA1 has inframe fused GFP replacing the N terminus of EBNA1.

Acknowledgements Thanks to Daniela Quintana for contribution to cloning the line 26 junctional sequences, Goutham Subramanain for contribution to characterising the Rab28 genome region sequences in the line 26 and Maria Jackson who contributed to construction of the dnEBNA1 plasmids.

Author contributions SA conducted FACS experiments, western analyses and drug assays, YA-S cloned the line 59 transgene and contributed to FISH, DC and MD contributed to mouse work and cloning the line 26 transgene, AH conducted the dnEBNA1 analyses, SB supervised and analysed the FISH experiment, PH, AK and PL contributed to the RNA data (array and seq) analyses, KA contributed to the drug analyses, MB conducted the PD-L1 analysis, PT contributed to transgene cloning, the array experiment and mouse work. JBW devised, supervised and procured funding for the study and wrote the manuscript.

Funding Funding contribution to the work includes former LRF (now Bloodwise) grants. AH was supported by a Wellcome Trust PhD studentship while at GU, KA is supported by a PhD BBSRC studentship. SA is, and YA was, supported by Saudi Arabian PhD scholarships.

Compliance with ethical standards

Conflict of interest The authors declare that they have no conflict of interest.

References

1. Sivachandran N, Thawe NN, Frappier L. Epstein-Barr virus nuclear antigen 1 replication and segregation functions in nasopharyngeal carcinoma cell lines. J Virol. 2011;85:10425–30.
2. Canaan A, Haviv I, Urban AE, Schulz VP, Hartman S, Zhang Z, et al. EBNA1 regulates cellular gene expression by binding cellular promoters. Proc Natl Acad Sci USA. 2009;106:22421–6.
3. Deschamps T, Quentin B, Leske DM, MacLeod R, Mompelat D, Tafforeau L. Epstein-Barr Virus Nuclear Antigen 1 aEBNA1a interacts with Regulator of Chromosome Condensation aRCC1a dynamically throughout the cell cycle. J Gen Virol. 2017;98:251–265.
4. Malik-Soni N, Frappier L. Proteomic profiling of EBNA1-host protein interactions in latent and lytic Epstein-Barr virus infections. J Virol. 2012;86:6999–7002.
5. Gnanasundram SV, Pyndiah S, Daskalogianni C, Armfield K, Nylander K, Wilson JB, Fåhraeus R. PI3Kδ activates E2F1 synthesis in response to mRNA translation stress. Nat Commun. 2017;8:2103. in press
6. Wilson JB, Bell JL, Levine AJ. Expression of Epstein-Barr virus nuclear antigen-1 induces B cell neoplasia in transgenic mice. EMBO J. 1996;15:3117–26.
7. Kennedy G, Komano J, Sugden B. Epstein-Barr virus provides a survival factor to Burkitt's lymphomas. Proc Natl Acad Sci USA. 2003;100:14269–74.
8. Saridakis V, Sheng Y, Sarkari F, Holowaty MN, Shire K, Nguyen T, et al. Structure of the p53 binding domain of HAUSP/USP7 bound to Epstein-Barr nuclear antigen 1 implications for EBV-mediated immortalization. Mol Cell. 2005;18:25–36.
9. O'Neil JD, Owen TJ, Wood VH, Date KL, Valentine R, Chukwuma MB, et al. Epstein-Barr virus-encoded EBNA1 modulates the AP-1 transcription factor pathway in nasopharyngeal carcinoma cells and enhances angiogenesis in vitro. J Gen Virol. 2008;89:2833–42.
10. Owen TJ, O'Neil JD, Dawson CW, Hu C, Chen X, Yao Y, et al. Epstein-Barr virus-encoded EBNA1 enhances RNA polymerase III-dependent EBER expression through induction of EBER-associated cellular transcription factors. Mol Cancer. 2010;9:241.
11. Wood VH, O'Neil JD, Wei W, Stewart SE, Dawson CW, Young LS. Epstein-Barr virus-encoded EBNA1 regulates cellular gene transcription and modulates the STAT1 and TGFbeta signaling pathways. Oncogene. 2007;26:4135–47.
12. Tempera I, De Leo A, Kossenkov AV, Cesaroni M, Song H, Dawany N, et al. Identification of MEF2B, EBF1, and IL6R as direct gene targets of Epstein-Barr Virus (EBV) nuclear antigen 1 critical for EBV-infected B-lymphocyte survival. J Virol. 2015;90:345–55.
13. Drotar ME, Silva S, Barone E, Campbell D, Tsimbouri P, Jurvansu J, et al. Epstein-Barr virus nuclear antigen-1 and Myc cooperate in lymphomagenesis. International journal of cancer. J Int du Cancer. 2003;106:388–95.
14. Wilson JB, Levine AJ. The oncogenic potential of Epstein-Barr virus nuclear antigen 1 in transgenic mice. Curr Top Microbiol Immunol. 1992;182:375–84.
15. Tsimbouri P, Al-Sheikh Y, Drotar ME, Cushley W, Wilson JB. Epstein-Barr virus nuclear antigen-1 renders lymphocytes responsive to IL-2 but not IL-15 for survival. J Gen Virol. 2008;89:2821–32.
16. Tsimbouri P, Drotar ME, Coy JL, Wilson JB. bcl-xL and RAG genes are induced and the response to IL-2 enhanced in EμEBNA-1 transgenic mouse lymphocytes. Oncogene. 2002;21:5182–7.
17. Boyman O, Sprent J. The role of interleukin-2 during homeostasis and activation of the immune system. Nat Rev Immunol. 2012;12:180–90.
18. Li DQ, Divijendra Natha Reddy S, Pakala SB, Wu X, Zhang Y, Rayala SK, et al. MTA1 coregulator regulates p53 stability and function. J Biol Chem. 2009;284:34545–52.
19. Okoro DR, Rosso M, Bargonetti J. Splicing up mdm2 for cancer proteome diversity. Genes Cancer. 2012;3:311–9.
20. Schuster K, Fan L, Harris LC. MDM2 splice variants predominantly localize to the nucleoplasm mediated by a COOH-terminal nuclear localization signal. Mol Cancer Res. 2007;5:403–12.
21. Zheng T, Wang J, Zhao Y, Zhang C, Lin M, Wang X, et al. Spliced MDM2 isoforms promote mutant p53 accumulation and gain-of-function in tumorigenesis. Nat Commun. 2013;4:2996.
22. Rosso M, Okoro DE, Bargonetti J. Splice variants of MDM2 in oncogenesis. Subcell Biochem. 2014;85:247–61.
23. Bill KL, Garnett J, Meaux I, Ma X, Creighton CJ, Bolshakov S, et al. SAR405838: a novel and potent inhibitor of the MDM2:p53 axis for the treatment of dedifferentiated liposarcoma. Clin Cancer Res. 2016;22:1150–60.
24. Wade M, Li YC, Wahl GM. MDM2, MDMX and p53 in oncogenesis and cancer therapy. Nat Rev Cancer. 2013;13:83–96.
25. Gu L, Zhang H, Liu T, Zhou S, Du Y, Xiong J, et al. Discovery of dual inhibitors of MDM2 and XIAP for cancer treatment. Cancer Cell. 2016;30:623–36.
26. Zhang H, Gu L, Liu T, Chiang KY, Zhou M. Inhibition of MDM2 by nilotinib contributes to cytotoxicity in both Philadelphia-positive and negative acute lymphoblastic leukemia. PLoS ONE. 2014;9:e100960.
27. Kojima K, Burks JK, Arts J, Andreeff M. The novel tryptamine derivative JNJ-26854165 induces wild-type p53- and E2F1-mediated apoptosis in acute myeloid and lymphoid leukemias. Mol Cancer Ther. 2010;9:2545–57.
28. Renouf B, Hollville E, Pujals A, Tetaud C, Garibal J, Wiels J. Activation of p53 by MDM2 antagonists has differential apoptotic effects on Epstein-Barr virus (EBV)-positive and EBV-negative Burkitt's lymphoma cells. Leukemia. 2009;23:1557–63.
29. Kang MS, Lu H, Yasui T, Sharpe A, Warren H, Cahir-McFarland E, et al. Epstein-Barr virus nuclear antigen 1 does not induce

lymphoma in transgenic FVB mice. Proc Natl Acad Sci USA. 2005;102:820–5.
30. Goodman A, Patel SP, Kurzrock R. PD-1-PD-L1 immune-checkpoint blockade in B-cell lymphomas. Nat Rev Clin Oncol. 2017;14:203–20.
31. Xie N, Ma L, Zhu F, Zhao W, Tian F, Yuan F, et al. Regulation of the MDM2-p53 pathway by the nucleolar protein CSIG in response to nucleolar stress. Sci Rep. 2016;6:36171.
32. Zhang Z, Wang H, Li M, Rayburn ER, Agrawal S, Zhang R. Stabilization of E2F1 protein by MDM2 through the E2F1 ubiquitination pathway. Oncogene. 2005;24:7238–47.
33. Tian X, Chen Y, Hu W, Wu M. E2F1 inhibits MDM2 expression in a p53-dependent manner. Cell Signal. 2011;23:193–200.
34. Volk EL, Fan L, Schuster K, Rehg JE, Harris LC. The MDM2-a splice variant of MDM2 alters transformation in vitro and the tumor spectrum in both Arf- and p53-null models of tumorigenesis. Mol Cancer Res. 2009;7:863–9.
35. Zimber-Strobl U, Strobl L, Hofelmayr H, Kempkes B, Staege MS, Laux G, et al. EBNA2 and c-myc in B cell immortalization by Epstein-Barr virus and in the pathogenesis of Burkitt's lymphoma. Curr Top Microbiol Immunol. 1999;246:315–20. discussion 321
36. Wilson JB, Drotar ME. Considerations in generating transgenic mice. DNA, RNA, and protein extractions from tissues--rapid and effective blotting. Methods Mol Biol. 2001;174:361–77.
37. Hannigan A, Wilson JB. Evaluation of LMP1 of Epstein-Barr virus as a therapeutic target by its inhibition. Mol Cancer. 2010;9:184.
38. Achilli F, Boyle S, Kieran D, Chia R, Hafezparast M, Martin JE, et al. The SOD1 transgene in the G93A mouse model of amyotrophic lateral sclerosis lies on distal mouse chromosome 12. Amyotroph Lateral Scler Other Mot Neuron Disord. 2005;6:111–4.
39. Croft JA, Bridger JM, Boyle S, Perry P, Teague P, Bickmore WA. Differences in the localization and morphology of chromosomes in the human nucleus. J Cell Biol. 1999;145:1119–31.